QuantumSi

# Control More of Your Protein Research

## Introducing Platinum™ – The World's First *Next-Generation* Protein Sequencer

The power of protein sequencing is now in your hands! Sequence proteins right in your lab with Platinum™, the NEW benchtop solution from Quantum-Si.

Our first-of-its-kind platform gives you the power to take more control of your protein research by conveniently delivering simple, affordable protein sequencing capabilities right to your bench, without the need for bioinformatics expertise or extensive infrastructure. Now you can get deeper insights into protein biology to complement your existing proteomics approaches...right in your lab!

- Conduct proteomics experiments in your lab *at your bench*
- Interrogate protein variants and modifications, and correlate with biological function
- Achieve deeper proteomics insights faster
- Perform analytics with no bioinformatics expertise required

Introducing Platinum™

The Protein Sequencing Company™

DOI 10.1002/pmic.201300084 *Proteomics* 2014, *14*, 1480–1493

RESEARCH ARTICLE

# Mechanisms of kidney repair by human mesenchymal stromal cells after ischemia: A comprehensive view using label-free MS$^E$

*Milene R. da Costa*[1,2*,**], *Luciana Pizzatti*[3,4*,***], *Rafael S. Lindoso*[1,2], *Julliana Ferreira Sant'Anna*[1,2], *Barbara DuRocher*[3,4], *Eliana Abdelhay*[3,4] *and Adalberto Vieyra*[1,2]

[1] Carlos Chagas Filho Institute of Biophysics, Federal University of Rio de Janeiro, Rio de Janeiro, Brazil
[2] National Institute of Science and Technology for Structural Biology and Bioimaging, Rio de Janeiro, Brazil
[3] National Institute of Cancer, Rio de Janeiro, Brazil
[4] Proteomic Network of Rio de Janeiro, Brazil

Received: February 26, 2013
Revised: February 24, 2014
Accepted: March 27, 2014

Acute kidney injury (AKI) is one of the more frequent and lethal pathological conditions seen in intensive care units. Currently available treatments are not totally effective but stem cell-based therapies are emerging as promising alternatives, especially the use of mesenchymal stromal cells (MSC), although the signaling pathways involved in their beneficial actions are not fully understood. The objective of this study was to identify signaling networks and key proteins involved in the repair of ischemia by MSC. Using an in vitro model of AKI to investigate paracrine interactions and label-free high definition 2D-NanoESI-MS$^E$, differentially expressed proteins were identified in a human renal proximal tubule cell lineage (HK-2) exposed to human MSC (hMSC) after an ischemic insult. In silico analysis showed that hMSC stimulated antiapoptotic activity, normal ROS handling, energy production, cytoskeleton organization, protein synthesis, and cell proliferation. The proteomic data were validated by parallel experiments demonstrating reduced apoptosis in HK-2 cells and recovery of intracellular ATP levels. qRT-PCR for proteins implicated in the above processes revealed that hMSC exerted their effects by stimulating translation, not transcription. Western blotting of proteins associated with ROS and energy metabolism confirmed their higher abundance in HK-2 cells exposed to hMSC.

**Keywords:**
Acute kidney injury / Label-free quantification / Mesenchymal stromal cells / Paracrine communication / Signal transduction pathways / Technology

Additional supporting information may be found in the online version of this article at the publisher's web-site

## 1 Introduction

Acute kidney injury (AKI) is a major health issue that affects up to 20% of hospitalized patients [1]. The condition is associated with late development of chronic renal disease, high mortality, and inevitably increased health expenditure.

**Correspondence**: Professor Adalberto Vieyra, Instituto de Biofísica Carlos Chagas Filho, Av Carlos Chagas Filho, 373, Universidade Federal do Rio de Janeiro, 21941 Rio de Janeiro, Brazil
**E-mail**: avieyra@biof.ufrj.br
**Fax**: +55-21-2280-8193

**Abbreviations**: **AKI**, acute kidney injury; **BAD**, Bcl-2-associated death promoter; **HK-2**, human renal proximal tubule cell lineage; **hMSC**, human mesenchymal stromal cells; **MSC**, mesenchymal stromal cells; **MS$^E$**, high resolution label-free MS with data-independent scanning; **NanoUPLC**, nano-ultra-high pressure chromatography; **SCX**, strong cation exchange

*These authors contributed equally to this work.
**Current address: Faculty of Pharmacy, Federal University of Rio de Janeiro, Rio de Janeiro, Brazil.
***Current address: Chemistry Institute, Federal University of Rio de Janeiro, Rio de Janeiro, Brazil.

Since there is no definitive or completely effective treatment to prevent impairment of renal function or improve patient recuperation [1, 2], much effort has been concentrated on the development of alternative treatments such as stem cell-based therapies [3, 4].

Among the different types of stem cells investigated as candidates for cell therapies, mesenchymal stromal cells (MSC) have received special attention. Their use in treating neurological, immunological, cardiac, and renal diseases has been extensively explored [5]. MSC are multipotent cells present in adult organisms and are capable of differentiating into specialized cells, e.g. osteoblasts, chondrocytes, adipocytes, and others [6]. The most common sources of MSC are the bone marrow and adipose tissue [7], but other organs such as the kidney have their own niches of MSC-like cells [8].

Besides their broad distribution in the body and ease of isolation, interest in MSC was originally stimulated by their capacity to differentiate into other cell types, suggesting that they could be a source of healthy cells to repair/replace injured tissue [9]. There is substantial evidence from both in vitro studies and animal models of AKI that MSC can promote and/or improve regenerative responses in the injured kidney, leading to tissue repair and recuperation of renal function [10–12]. However, few MSC remain in the kidney after a deleterious insult, making the hypothesis that they fuse or transdifferentiate into renal cells unlikely to explain their protective effects [13, 14]. There is now strong evidence that the beneficial effects of MSC are attributable to paracrine mechanisms, i.e. local secretion of biologically active molecules that modulate tissue responses to an insult [15]. Together, these trophic factors trigger antiapoptotic, immunomodulatory, antiscarring, and angiogenic responses, which culminate in tissue repair [5, 16].

Despite the knowledge that has accumulated about the potential therapeutic effects of MSC, the specific molecular-level changes they cause in injured renal cells are still not fully understood. Therefore, the focus of this study was to identify key proteins and metabolic/signaling pathways regulated by human MSC (hMSC) in human renal proximal tubule cells after ischemic injury, especially those contributing to the protective effects of hMSC. Using an in vitro model of AKI and label-free high definition 2D-NanoESI-MS$^E$, we were able to identify differentially expressed proteins in a human renal proximal tubule cell lineage (HK-2) exposed to hMSC after the insult. Subsequent in silico analysis revealed the biochemical pathways and cellular processes modulated, providing evidence that hMSC affect important cellular processes culminating in repair.

## 2 Materials and methods

### 2.1 Human kidney (HK-2) cell cultures

Immortalized HK-2 cells (CRL-2190; ATCC, Manassas, VA, USA), a proximal tubule cell lineage, were grown in 75-cm$^2$ cell culture flasks containing DMEM supplemented with penicillin (100 U/mL), streptomycin (100 μg/mL), and 10% FBS, all purchased from Invitrogen$^{TM}$, Life Technologies (Carlsbad, CA, USA). The cells were maintained at 37°C in 100% humidified air containing 5% $CO_2$.

### 2.2 Human mesenchymal cells (hMSC): Isolation and culture

Bone marrow samples were obtained from healthy donors after written informed consent, according to the guidelines of the local ethics committee (National Institute of Cancer, Rio de Janeiro, Brazil). hMSCs isolated from heparinized bone marrow samples as previously described [17] were grown in low glucose DMEM supplemented with 10% FBS (HyClone®, Waltham, MA, USA), 2 mM glutamine, 100 U/mL penicillin and 100 μg/mL streptomycin (Invitrogen$^{TM}$) and incubated as described above. One half of the medium was changed twice a week until 80–90% confluence had been reached (approximately 10 days). The cells were harvested with 0.1% trypsin and replicated at $2 \times 10^5$ cells/cm$^2$ in medium as above.

### 2.3 In vitro model of acute renal injury

We used a well-established in vitro model of acute renal injury based on glucose and ATP depletion [18–20]. A total of $10^6$ HK-2 cells from the cultures described in Section 2.1 were transferred to a 55 cm$^2$ cell culture dish containing 10 mL supplemented DMEM. Cells were cultured for 72 h until 80% confluence, rinsed twice with PBS and the medium replaced with Hank's balanced salt solution containing 1.3 mM $CaCl_2$, 0.8 mM $MgCl_2$, 50 μM antimycin A (an inhibitor of the mitochondrial electron transport complex III) and 10 mM 2-deoxyglucose (a nonmetabolizable analog of D-glucose that inhibits glycolysis), both purchased from Sigma-Aldrich (Saint Louis, MO, USA). After 30 min, the solution was discarded and the cells were rinsed twice with PBS to remove the inhibitors. In order to mimic an in vivo "reperfusion" by reexposure to normal metabolic conditions, 10 mL low glucose DMEM (not supplemented with FBS) were added to the culture dish, which was maintained at 37°C in the atmosphere described above for a 3-h "recovery period."

### 2.4 Coculture of HK-2 cells with hMSC during recovery period

To assess the influence of hMSC on protein expression in HK-2 cells, the two types of cells were cocultured during the recovery period. For this purpose, a permeable support system (Transwell®, Corning, Tewksbury, MA, USA) with a 0.4 μm porous membrane was fitted into the 55 cm$^2$ culture dish containing HK-2 cells that had been ATP- and

 

glucose-deprived, as described in Section 2.3 above, and then 6 mL of low glucose DMEM (not supplemented with FBS) containing $10^6$ hMSC were layered on the upper surface of the support. The permeable membrane of the coculture system ensures that the two cell populations remain physically separated, but they can communicate through the release of soluble factors into the culture medium [21, 22]. After the recovery period (3 h) the insert was carefully removed to avoid cross-contamination and only the HK-2 cells were analyzed.

### 2.5 Coculture of HK-2 cells with human fibroblasts (hFB) during the recovery period

Human fibroblasts (HFF-1; Rio de Janeiro Cell Bank, Rio de Janeiro, Brazil) were used instead of hMSC in control experiments to determine whether they could influence renal cell death and intracellular ATP content. These cells were grown in 75 $cm^2$ culture flasks containing low glucose DMEM supplemented with penicillin (100 U/mL), streptomycin (100 μg/mL), and 10% FBS, all purchased from Invitrogen™, Life Technologies. hFB were maintained at 37°C in a 100% humidified air containing 5% $CO_2$ until use. HK-2 cells (initially $10^6$ cells cultured for 72 h until they reached 80% confluence) and hFB ($10^6$ cells per transwell) were cocultured as described in Section 2.4.

### 2.6 Protein extraction and in-solution tryptic digestion

A total of four 55 $cm^2$ cell culture dishes containing HK-2 cells subjected to ATP depletion and then cocultured with hMSC, as described in Sections 2.3 and 2.4, were harvested with 0.1% trypsin and washed twice with PBS, and proteins were extracted immediately [23]. This procedure was repeated on HK-2 cells subjected to ATP depletion but not cocultured with hMSC. All experiments were performed in triplicate. Briefly, the collected cells were resuspended in 100 μL cold lysis buffer containing 50 mM Tris-HCl (pH 7.5), 5 mM EDTA, 10 mM EGTA, 50 mM NaF, 20 mM KCl, 250 mM NaCl supplemented with 1 μL protease inhibitor cocktail (GE Healthcare, Life Sciences, Piscataway, NJ, US) and phosphatase inhibitors (20 mM sodium orthovanadate ($Na_3VO_4$) and 1 μM okadaic acid). After 1 h at 4°C, the suspension was frozen and thawed twice in liquid $N_2$. The total extracts were centrifuged at 12 000 × *g* for 30 min and the supernatants were collected for storage at –80°C.

After Bradford quantification of protein, the samples were concentrated 39× and exchanged with 50 mM $NH_4HCO_3$ using a 3-kDa ultra-filtration device (Millipore, Billerica, MA, USA). A total of 200 μg of protein were denatured (0.1% *Rapi*GEST SF at 60°C for 15 min) (Waters, Milford, MA, USA), reduced with 10 mM DTT at 60°C for 30 min, alkylated with 10 mM iodoacetamide for 30 min at room temperature in the dark and enzymatically digested with trypsin at a 1:50 w/w enzyme/protein ratio (Promega, Madison, WI, USA). Digestion was stopped by adding 10 μL 5% TFA, and yeast alcohol dehydrogenase (ADH; P00330, Waters) was added to the digests to a final concentration of 10 fmol/uL as an internal standard for absolute quantification [24, 25].

### 2.7 Label-free protein quantification by MS

Qualitative and quantitative nano-ultra-high pressure chromatography (nanoUPLC) tandem nanoESI-HDMS$^E$ experiments were conducted with a nanoACQUITY UPLC system (Waters) [26], but with slight modifications. For the first dimension, a 180 μm × 23 mm strong cation exchange (SCX) column (Waters) packed with 5 μm PolySULFOETHYL Aspartamide (PolyLC™, Columbia, MD, USA) was used. Typical on-column sample loads were 3 μg of protein digest for triplicate analyses. Samples were eluted in nine fractions from the SCX column using a salt gradient (2 μL salt plugs containing 50, 100, 150, and 200 mM ammonium formate ($NH_4FA$) with 5% ACN, followed by a RP gradient (2 μL organic plugs 10%, 20%, and 30% ACN with 200 mM $NH_4FA$, 30% ACN with 350 mM $NH_4FA$) and a flush. Each plug was loaded with loading buffer (5 mM $NH_4FA$, pH 3.2, containing 5% ACN) at 3 μL/min flow rate for 3 min [27]. The peptides released were captured by a downstream RP trap column (180 μm × 20 mm, 5 μm Symmetry C18, Waters). After all the peptides had been captured, the trap column was placed online with another RP analytical column (100 μm × 100 mm, 1.8 μm C18, nanoACQUITY UPLC HSS T3, Waters). A RP gradient 5–40% ACN (containing 0.1% v/v formic acid) in 58 min was used for the second dimension at a flow rate of 600 nL/min.

All analyses were performed using nano-electrospray ionization in the positive ion mode nanoESI (+) and a NanoLockSpray ionization source (Waters). The lock mass channel was sampled every 30 s. The mass spectrometer was calibrated with a MS/MS spectrum of [Glu$^1$]-Fibrinopeptide B human (Glu-Fib) solution (Sigma-Aldrich) (100 fmol/mL) delivered through the reference sprayer of the NanoLockSpray source. The doubly-charged ion ($[M + 2H]^{2+} = 785.8426$) was used for initial single-point calibration and MS/MS fragment ions of Glu-Fib were used for the final instrument calibration. Multiplexed data-independent (DIA) scanning with added specificity and selectivity of a nonlinear "T-wave" ion mobility (HDMS$^E$) experiments were performed with a Synapt HDMS mass spectrometer (Waters) [23]. The mass spectrometer switch between low collision energy MS (3 eV) and elevated collision energies MS$^E$ (high resolution label-free MS with data-independent scanning) (12–40 eV) applied to the trap "T-wave" CID cell with argon; the transfer "T-wave" collision cell was adjusted to 1 eV, using a scan time of 1 s, at both low and high energies, providing a minimum of 10 points above 10% peak capacity. Full-scan orthogonal acceleration TOF (*oa*-TOF) MS$^E$ was acquired from *m/z* 50 to 2000. The MS profile was tuned to guarantee that the low energy

 

LC/MS data were effectively acquired from $m/z$ 400 to 2000, ensuring that all masses $<m/z$ 400 in the LC/MS$^E$ arose from dissociations in the collision cell in the second total ion count channel of the mass spectrometer.

### 2.8 Database searching and quantification

Database searching and quantification were as previously described [23]. Protein identification and quantitative data packaging were generated by appropriate algorithms [27, 28] and searching against a human-specific database. The databases used were randomised "on-the fly" during database queries, and appended to the original database to access the false-positive rate of identification [29]. For appropriate spectral processing and database searching conditions, a ProteinLynxGlobalServer v.2.5.2 (PLGS) with Expression$^E$ informatics v.2.5.2 was used. UniProtKB (release 2011_11) with manually reviewed annotations was used, and search conditions were based on taxonomy (*Homo sapiens*), maximum missed cleavages by trypsin allowed up to 1, variable modifications by carbamidomethyl (C) and acetyl N-terminal and oxidation (M) [30]. Only those proteins that were identified in all replicates during the Identity$^E$ step of PLGS analysis were considered in the expression analysis performed by Expression$^E$ tool.

Protein interactions were analyzed using Ingenuity Pathway Analysis software (IPA-http://www.ingenuity.com) and GeneGO MetaCore software (GeneGO, Encinitas, CA). For network analysis, transcription regulation, and direct interactions, the workflow tool was used.

### 2.9 Analysis of renal cell death and intracellular ATP assay

To evaluate the paracrine influence of hMSC on renal cell death and intracellular ATP content after ATP and glucose depletion (Section 2.3), the two cell populations were cocultured as described in Section 2.4. The HK-2 cells were harvested with 0.1% trypsin (Invitrogen$^{TM}$), washed twice with PBS and immediately used for cell death analysis and intracellular ATP assay. In parallel assays, ATP content and renal cell death were also evaluated in: (i) HK-2 cells not subjected to respiration blockade; (ii) HK-2 cells treated with antimycin A to block mitochondrial respiration and ATP synthesis followed by a 3-h recovery period; (iii) HK-2 cells treated with antimycin A, washed and cocultured with hMSC during the 3-h recovery period; (iv) HK-2 cells treated with antimycin A, washed and cocultured with hFB during the 3-h recovery period.

For the renal cell death assays, a total of $10^5$ cells were suspended in binding buffer (10 mM HEPES, 140 mM NaCl, and 2.5 mM $CaCl_2$; pH 7.4) to a final volume of 100 μL, and incubated in the dark with 5 μL Annexin V-Alexa Fluor$^{TM}$ (Invitrogen$^{TM}$) for 15 min at room temperature. Propidium iodide (1.5 μM final concentration; Sigma-Aldrich) was added and the samples were placed on ice for immediate analysis. Cell death was evaluated using a flow cell based bench top FACS Calibur Cytometer (BD Biosciences, Billerica, MA, USA).

Intracellular ATP was assayed by the luciferase and luciferin method [31]. A 100 μL aliquot containing $10^5$ cells was mixed with 100 μL somatic cell ATP releasing reagent (Sigma-Aldrich) and immediately treated with the bioluminescent ATP assay kit (FLASC, Sigma-Aldrich).

### 2.10 Quantitative real-time PCR

RNA transcripts were quantified using real-time PCR. Four micrograms of RNA extracted from HK-2 cells with Trizol (Invitrogen) were reverse-transcribed with the ImProm-II$^{TM}$ Reverse Transcription System (Promega, Madison, WI, USA). The cDNAs were mixed with SYBR Green PCR Master Mix® (Applied Biosystems, Foster City, CA, USA) and target genes of pyruvate kinase, malate dehydrogenase, succinate dehydrogenase A and B, $F_0F_1$-ATP synthase α and β-subunits, peroxiredoxin 1 and 6, cofilin 1, profilin 1, septin 7, and β-actin. Real-time PCR was performed with 45 cycles of 15 s at 95°C and 1 min at 60°C in an ABI Prism 7000 thermocycler (Applied Biosystems, Foster City, CA, USA). The expression level of each sample was estimated from triplicate experiments with specific and control primers. The amounts of the target gene and internal control (β-actin) transcripts were estimated using a standard curve. The fold change in expression was calculated using the $2^{-(\Delta\Delta Ct)}$ method, the values being expressed in arbitrary units as the fold increase of the target gene transcript under AR or AR + hMSC conditions compared to normal cells (data represented by means ± SD). The primer sequences are available upon request.

### 2.11 Western blotting

The proteomic data were further validated by Western blotting of key proteins in pathways associated with ROS handling and energy metabolism. The following antibodies were used: polyclonal ab59543 for peroxiredoxin 6 (1:500 dilution), polyclonal ab96193 for malate dehydrogenase 2 (1:1000 dilution), and monoclonal ab14730 for FoF1-ATPsynthase β-subunit (1:500 dilution), all purchased from Abcam (Cambridge, MA, USA); polyclonal #3186 for pyruvate kinase isoforms 1 and 2 (1:1000 dilution) purchased from Cell Signaling Technology (Danvers, MA, USA). The secondary antibodies were goat anti-rabbit IgG-HRP sc-2030 and donkey anti-mouse IgG-HRP sc-2318, Santa Cruz Biotechnology (both at 1:2000). ImageJ software (http://rsbweb.nih.gov/ij/) was used for immunosignaling quantification.

### 2.12 Statistical analysis

Statistical analyses are described in the figure legends. GraphPad Prism version 6.0 Demo version (GraphPad Software, San Diego, CA, USA) was used.

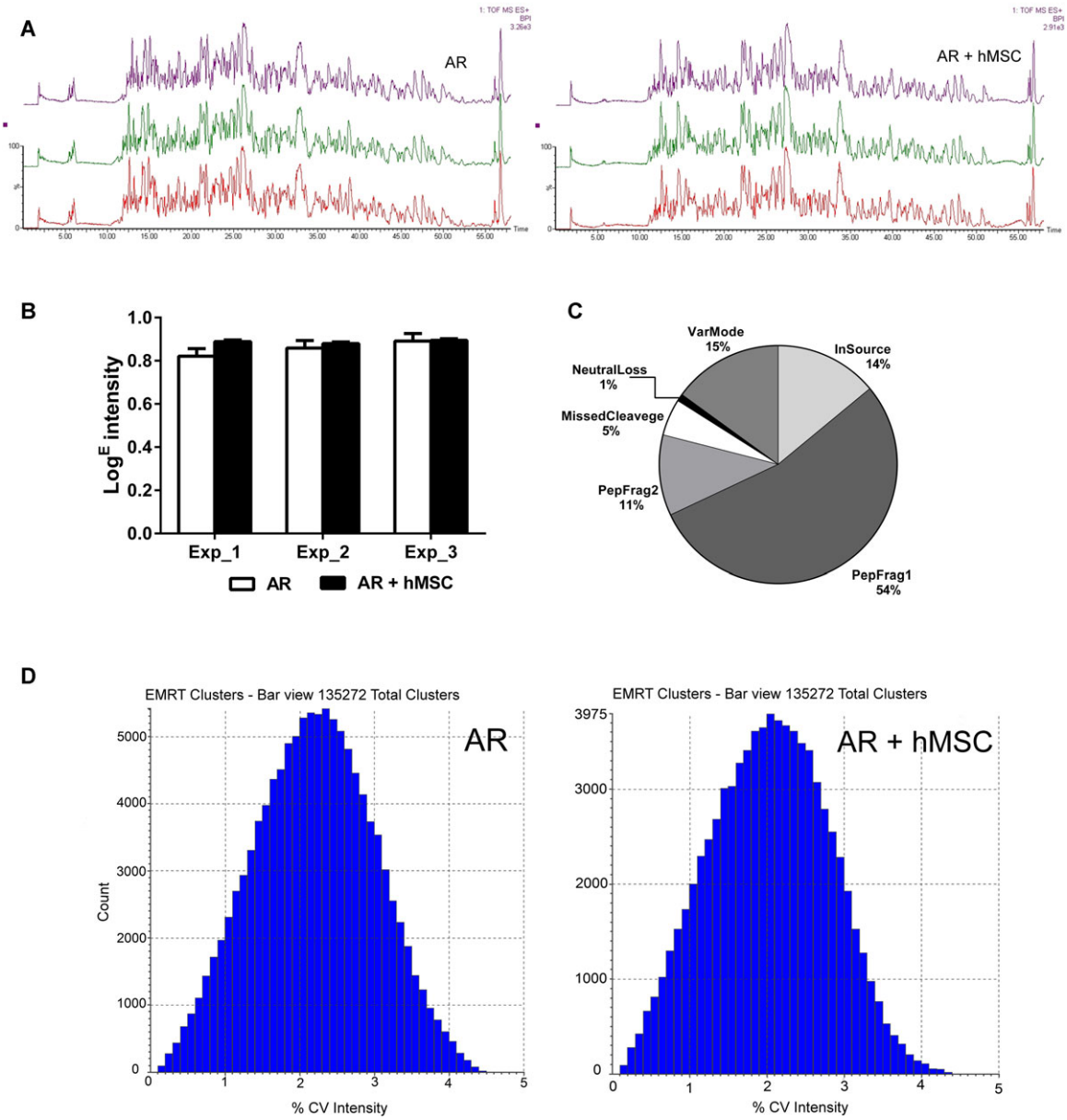


**Figure 1.** Label-free proteomic analysis. (A) Bidimensional chromatographic distribution of HK-2 renal cells under AR and AR + hMSC conditions. Traces indicate injections in triplicate. (B) Log$^E$ intensity plot of three replicate injections. (C) Peptide match distribution of the identified peptides. PepFrag1 and PepFrag2: peptide matches compared to database by PLGS; VarMod: variable modifications; InSource: fragmentation that occurred on ionization source; MissedCleavage: missed cleavage by trypsin; Neutral loss: water precursor loss. (D) Coefficient of variation plots of exact mass retention time (EMRT) for the triplicates in the two conditions.

## 3 Results

### 3.1 Human mesenchymal stromal cells induce modifications in the global protein expression of injured renal cells

To investigate the mechanisms underlying the therapeutic effects of hMSC in treating AKI, the global proteome of human renal cells (HK-2) subjected to chemical anoxia followed by a 3-h recovery period (anoxia → reoxygenation condition, AR) was compared with that of renal cells subjected to anoxia and cocultured with hMSC during the recovery period (AR + hMSC condition). The proteins from both conditions were identified using label-free protein quantification by MS (Sections 2.7 and 2.8). The identified proteins were organized by the PLGS Expression$^E$ tool algorithm into a list of those with significantly different expression levels in the AR + hMSC condition compared to the AR condition. The bidimensional chromatographic distribution using the SCX and RP set-ups is given in Fig. 1A.

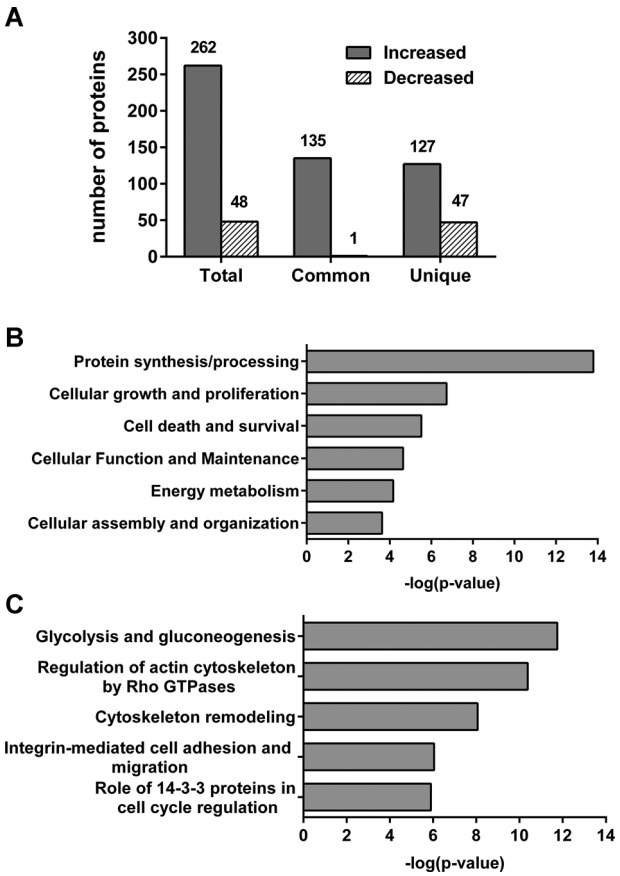


**Figure 2.** (A) Differential expression analysis obtained with Expression$^E$ indicating higher or lower protein levels in renal cells after chemical anoxia and coculturing with hMSC for 3 h (AR + hMSC) than in renal cells subjected to similar conditions, but not exposed to hMSC during the 3-h recovery period (AR). Common: proteins detected under both conditions. Unique: proteins detected under only one condition. (B) In silico analysis showing the six top GO processes. (C) In silico analysis showing six top biological pathways. *p*-value: the probability of the association between the cellular function and the upregulated protein being random.

More than 8000 peptides were identified, 5047 in AR and 4077 in AR + hMSC. The complete list of proteins and peptides confidentially identified among the six runs (three for each experimental condition) is presented in the Supporting Information Tables S1 and S2. The exact mass accuracy for 85% of the precursor ions demonstrates the distribution at a minimum of 15 ppm and the fragment ions at 5 ppm. The Log$^E$ intensities of the exact mass retention (EMRT) clusters obtained for both conditions are shown in Fig. 1B. The CV for the 135 272 EMRT clusters was <4 under both conditions (Fig. 1D). Approximately 6000 peptides were used for absolute quantification at the peptide level and the protein sequence coverage distribution was consistent with the EMRT clusters in our model (Supporting Information Fig. S1). The peptide match distribution demonstrates that 14% of the peptides were in source and that most identifications were consistent with the fragmentation in the trap CID cell (Fig. 1C). The dynamic range of quantified proteins under both conditions was consistent with the instrument used, covering a three Log dynamic range without ion mobility (Supporting Information Fig. S2).

High-throughput proteomic screening identified 553 proteins (236 in AR and 317 in AR + hMSC), of which 310 were differentially expressed between the two conditions. Among these, 262 were higher or unique in AR + hMSC and 48 were lower or not detected (Fig. 2A—see Supporting Information Table S3 for a complete list of the differentially expressed proteins, with annotations and quantification information).

### 3.2 In silico analysis reveals key cellular processes regulated by hMSC after ischemia

In silico analysis was performed with both IPA and MetaCore software (Section 2.8) to identify the cellular processes represented by the dataset of proteins differentially expressed in the ischemic renal cells cocultured with hMSC (AR + hMSC) during the recovery period. Both upregulated and downregulated proteins were analyzed simultaneously. Statistically validated IPA analysis uncovered the top cellular processes, some of which are particularly interesting in the context of AKI (Fig. 2B). These include protein synthesis/processing; cellular growth and proliferation; cell death and survival; cellular function and maintenance; energy metabolism; and cellular assembly and organization. The top cellular pathways identified (Fig. 2C) include glycolysis and gluconeogenesis (Supporting Information Fig. S3), cytoskeletal remodeling (Supporting Information Fig. S4), and role of 14–3–3 proteins in cell-cycle regulation (Supporting Information Fig. S5; for legends to MetaCore symbols see Supporting Information Fig. S6).

### 3.3 hMSC promote kidney cell survival, restore intracellular ATP, and stimulate protein translation

In silico analyses indicated the important cellular processes that might participate in the therapeutic actions of hMSC. Among these, we chose to investigate processes critical for the recuperation of renal cells after anoxia, which include cell death and survival, energy metabolism, and protein synthesis/processing. For this purpose, we used different orthogonal strategies: (i) annexin V/propidium iodide FACS to follow the influence of hMSC on cell death; (ii) chemical measurement of intracellular ATP to assess their effect on energy metabolism; (iii) qRT-PCR of mRNAs to examine their influence on the transcription of representative proteins.

During ischemia (AR condition) the percentage of apoptotic renal cells was ~fivefold higher than in normal cells (Fig. 3A and B). However, exposure to hMSC during the recovery period (AR + hMSC) decreased the number of

 

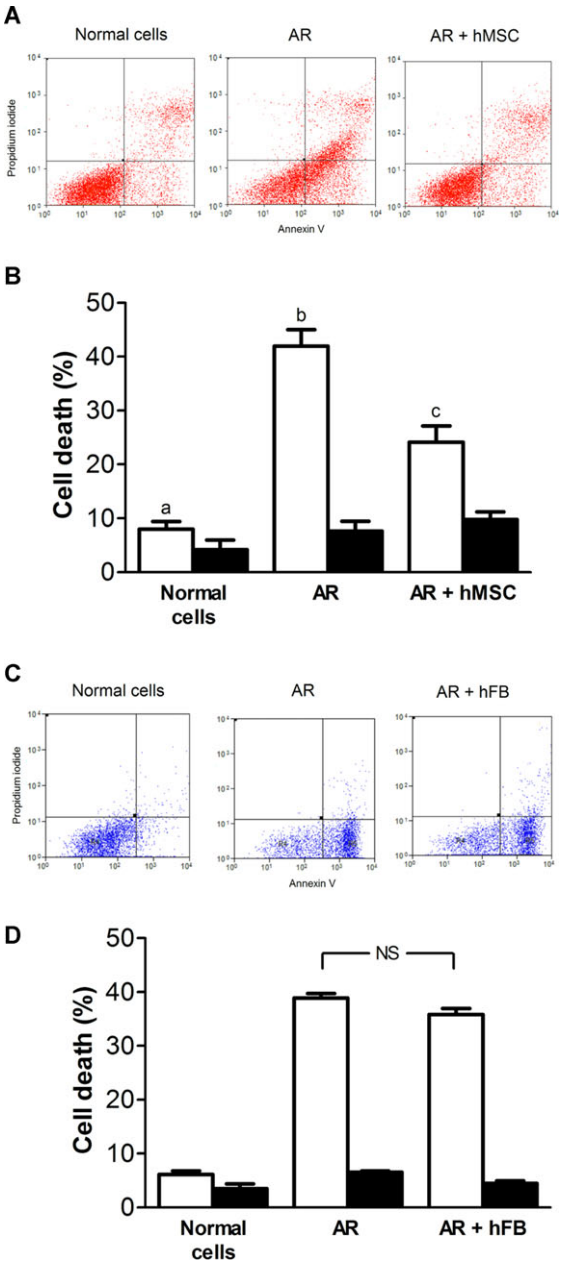


**Figure 3.** Representative cytometry for HK-2 cell death analyses with hMSC (A) or hFB (C). (B) and (D) Graphic representation of the percentage of apoptotic (empty bars) and necrotic (black bars) cells. The results are mean ± SEM of three determinations performed in triplicate using different renal cell cultures and different samples of hMSC originated from three donors. Different lower case letters above the bars indicate statistically different means ($p < 0.05$) (one-way ANOVA, followed by Newman–Keuls test). NS: No significant difference was found between AR and AR + hFB. No differences between conditions were found in necrotic cells. Normal cells: HK-2 cells not subjected to respiration blockade; AR: HK-2 cells treated with antimycin A to block mitochondrial respiration and ATP synthesis followed by a 3-h recovery period; AR + hMSC: HK-2 cells treated with antimycin A, washed and cocultured with hMSC during the 3-h recovery period; AR + hFB: HK-2 cells treated with antimycin A, washed and cocultured with hFB during the 3-h recovery period.

apoptotic cells by >40%. Control experiments with hFB demonstrated that they have no significant protective effect on renal cells after ischemia (Fig. 3C and D). The difference in number of necrotic cells between the two groups was not statistically significant. The decrease in apoptotic cells in AR + hMSC could be explained by the upregulation of several proteins involved in cellular survival responses, as indicated by both proteomic and genomic ontology analyses (Supporting Information Table S3).

With respect to energy metabolism, the anticipated exhaustion of intracellular ATP content in AR was significantly prevented in the coculture (AR + hMSC) condition (Fig. 4A). The data suggest that hMSC augment the cellular capacity to produce ATP, probably by enhancing the protein machinery needed to maintain normal energy status in the renal cells. Again, control experiments demonstrated that hFB did not influence the intracellular ATP content of renal cells after ischemia (Fig. 4B).

We also wanted to assess the transcriptional status of mRNAs for some of the proteins involved in the above-mentioned cellular processes. Key proteins in energy metabolism (pyruvate kinase, malate dehydrogenase, succinate dehydrogenase A and B, and the α and β subunits of the $F_0F_1$-ATP synthase), ROS handling (peroxiredoxin 1 and 6) and cytoskeletal remodeling (cofilin 1, profilin 1, and septin 7) were chosen. qRT-PCR (Fig. 5A, B, and C) demonstrated that the mRNAs of all these proteins were notably increased in AR, but their levels returned to near normal in AR + hMSC.

Since the RNA levels were apparently inconsistent with the proteomic data, the latter were further validated by Western blotting of key proteins involved in pathways related to ROS handling and energy supply. Levels of the β subunit of $F_0F_1$-ATP synthase (Fig. 6A), malate dehydrogenase (Fig. 6B), peroxiredoxin 6 (Fig. 6C), and pyruvate kinase (Fig. 6D) were higher in HK-2 cells cocultured with hMSC.

## 4 Discussion

The central hypothesis of this work was that paracrine interactions between a human proximal tubule cell lineage especially sensitive to ischemic injury [32] and hMSC modulate the expression of key proteins involved in cellular regeneration after ischemia. To test this supposition, we applied a large-scale MS-based approach [33] using NanoUPLC and label-free quantification with $MS^E$ technologies. These techniques have the advantages of requiring only minute quantities of sample and accurately identifying a large number of proteins [34]. Unlike data-dependent acquisition, peptides, and corresponding fragment ions are acquired at the same time in $MS^E$, thereby avoiding partial sampling of chromatographic peaks, which significantly improves the quality of the data [35, 36]. This analytical strategy proved to be a valuable tool to investigate complex phenomena and allowed a comprehensive view of the events that occur in injured renal cells during their interaction with hMSC, providing new

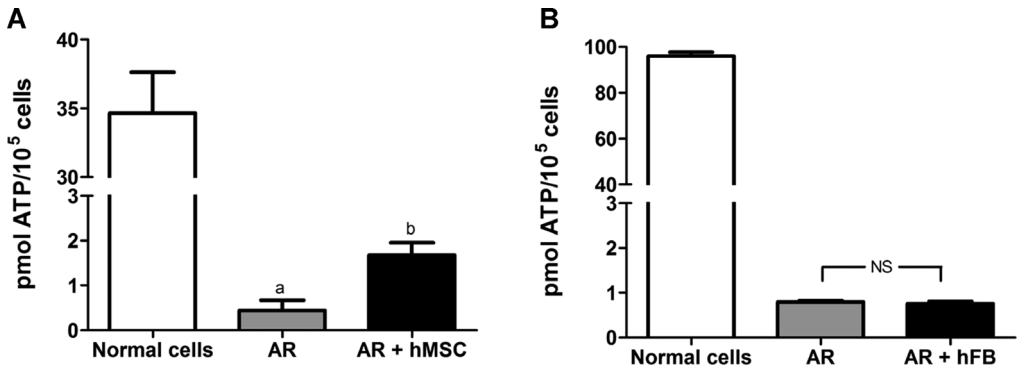


**Figure 4.** Intracellular ATP determinations in HK-2 cells. (A) With hMSC, (B) With hFB. The results are mean + SEM of three determinations performed in triplicate using different renal cell cultures and different samples of hMSC originated from three donors. Different lower-case letters above the bars indicate statistically different means ($p < 0.05$) (unpaired Student's *t*-test). NS: No significant difference between AR and AR + hFB. Normal cells: HK-2 cells not subjected to respiration blockade; AR: HK-2 cells treated with antimycin A to block mitochondrial respiration and ATP synthesis followed by a 3-h recovery period; AR + hMSC: HK-2 cells treated with antimycin A, washed and cocultured with hMSC during the 3-h recovery period; AR + hFB: HK-2 cells treated with antimycin A, washed and cocultured with hFB during the 3-h recovery period.

mechanistic insights about stem cells effects on different metabolic and signaling pathways in renal cells.

Differential proteomic analysis revealed that exposure to hMSC enhances the protein machinery necessary for renal cells to survive the deleterious consequences of ischemia-induced ATP depletion, which would otherwise lead to apoptosis and necrosis [37]. It should be emphasized that the substantial antiapoptotic paracrine effect of hMSC on renal cells (Fig. 3) matches the in silico analysis, which demonstrates that cellular processes linked to growth and proliferation—such as those given in Supporting Information Fig. S5—and to cell death and survival (Fig. 2B) are significantly represented in the ensemble of differentially expressed proteins. One of these proteins is BIRC-3 (baculoviral IAP repeat containing protein 3), also known as c-IAP2, which could only be detected in the treatment condition, indicating a strong influence of hMSC on its synthesis. BIRC-3 belongs to the human family of inhibitors of apoptosis proteins (IAP) [38]; it functions as an ubiquitin ligase targeting proapoptotic proteins (caspases 3, 7, and 9) for degradation [39]. BIRC-3 also participates in the signaling cascade that leads to activation of NF-κB, a transcriptional regulator of genes involved in cellular growth and inhibition of apoptosis [40], notably in ischemia [41].

The 14–3–3 group of proteins deserves special mention in the context of the antiapoptotic effects of hMSC (Fig. 3). These proteins modulate a broad spectrum of cell processes, notably by targeting hundreds of predominantly phosphorylated partner proteins that represent over 0.5% of the human proteome [42,43]. Also relevant from these analyses, the 14–3–3 proteins interfere with apoptosis through a variety of mechanisms that culminate in inhibition of the process [44]. In a recent publication [22] we demonstrated that bone marrow mononuclear cells prevent apoptosis in an ischemia reperfusion model in vivo, also preserving mitochondrial function, tubular structure, and key functional markers. It is therefore plausible that the beneficial influence of hMSC against apoptosis in HK-2 cells (Fig. 3) (in addition to those encountered in vivo [22]) involves the antiapoptotic properties of 14–3–3 proteins. The latter bind to phosphorylated Bcl-2-associated death promoter (BAD) [45, 46], helping to maintain it in the inactive form and consequently to slow the mitochondrial apoptotic pathway. Interestingly, Tögel et al. [47] demonstrated that MSC secrete survival factor insulin-like growth factor 1, which is known to promote the phosphorylation and inactivation of BAD [48]. Our proteomic studies support the view that the anti-apoptotic effects of MSC are due, in part, to the secretion of insulin-like growth factor 1 triggering the phosphorylation and inactivation of BAD, which occurs in conjunction with the upregulation of 14–3–3 proteins that help to keep it inactive.

Although identification of the 14–3–3 protein isoforms (Supporting Information Table S3) was based on a group of peptides, the list could show some redundancy. For example, when peptide DSTLIMQLLR is used to generate a list of identifications, we cannot accurately consider from which isoform this peptide is coming, or to which isoform the peptide quantification contributes most. This problem of protein inference, however, does not affect the main conclusion, that hMSC leads to the upregulation of an important protein involved in the antiapoptotic defenses of renal cells.

Other important participants in apoptosis are ROS, which are formed in substantial amounts and contribute significantly to the pathogenesis of several lesions encountered in AKI [49]. Supporting Information Table S3 demonstrates that coculture of HK-2 cells with hMSC also leads to upregulation of key enzymes implicated in ROS and redox handling as a whole, including NO, with impairment of apoptotic pathways: thioredoxin and peroxiredoxins 1 and 6. Thioredoxins belong to a family of proteins that catalyze the denitrosylation of *S*-nitrosylated proteins and trans-nitrosylation of other enzymes, as with caspase 3 [50]. Peroxiredoxin 6

 

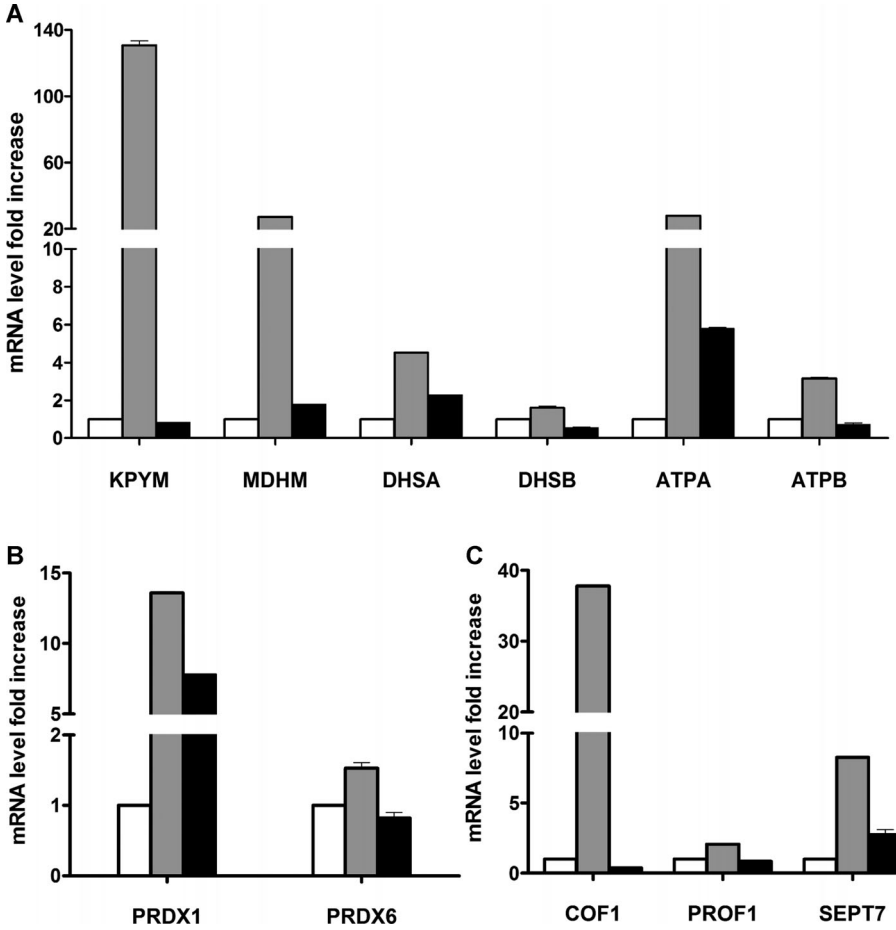


**Figure 5.** qRT-PCR analysis. (A) Energy metabolism. (B) ROS handling. (C) Cytoskeleton remodeling. Normal cells: HK-2 cells not subjected to respiration blockade (empty bars); AR: HK-2 cells treated with antimycin A to block mitochondrial respiration and ATP synthesis followed by a 3-h recovery period (gray bars); AR + hMSC: HK-2 cells treated with antimycin A, washed and cocultured with hMSC during the 3-h recovery period (black bars). Abbreviations: KPYM, pyruvate kinase; MDHM, malate dehydrogenase; DHSA/B succinate dehydrogenase A and B isoforms; ATPA/B, FoF1-ATP synthase α and β subunits; PRDX1/6, peroxiredoxin 1 and 6 isoforms; COF1, cofilin 1; PROF1, profilin 1; SEPT7, septin 7.

(upregulated ~two fold with respect to the AR condition) catalyzes the reduction of hydroperoxides [51], thus decreasing the local superoxide anion ($O_2^{-\cdot}$) concentration. Therefore, differential proteomics analysis supports the hypothesis that hMSC induces cooperative and simultaneous upregulation of two proteins in renal cells subjected to chemical anoxia in a process that culminates in the reduction of both $O_2^{-\cdot}$ and NO, and consequently in lower local formation of deleterious peroxynitrite ($ONOO^-$). This anion has been implicated in the nitration and indiscriminate inactivation of proteins, making it a potent inducer of cell death [52]. Recently, we demonstrated that stem cells strongly decrease ROS formation and stimulate *S*-nitrosylation of high-molecular mass proteins in renal mitochondria subjected to ischemia/reperfusion, as in cultured renal cells injured with antimycin A [22]. The present proteomic analysis allows us to hypothesize that the mechanisms involved in this key signaling/detoxification process underlie, at least in part, the MSC-induced upregulation of thioredoxin and peroxiredoxins 1 and 6.

Recovery from AKI requires restoration of ATP generation, an especially critical task in the organ with the greatest respiratory demand in humans [53]. We previously demonstrated that stem cells can preserve ATP synthesis in mitochondria after ischemia/reperfusion [22], which is consistent with the significant recovery of intracellular ATP levels in HK-2 cells cocultured with hMSC (Fig. 4). Furthermore, in view of the results of the present proteomic study, we propose that the marked upregulation of $F_0F_1$-ATP synthase β-subunit (Supporting Information Table S3), which participates directly in the catalysis of ATP synthesis, plays a structural role in the beneficial effects of stem cells on this process. Parallel upregulation of cytochrome *c* in renal cells by hMSC cooperates with augmented ATP generation because this protein conveys electrons to the final step of the mitochondrial electron transport chain [54], thereby maintaining full respiratory function. It could be argued that the low levels of intracellular ATP recovered after treatment with hMSC (Fig. 4) would not be enough to meet the physiological demands of cells recovering from anoxia. However, we propose that the lower steady levels of ATP reflect very high turnover, which underpins the multiple cell functions involved in accelerated recovery. This is supported by the marked hMSC-induced reduction in the number of apoptotic cells (Fig. 3), which would not be observed if the ATP supply was insufficient.

However, ATP synthesis also requires reduced species to feed the respiratory chain and generate a mitochondrial

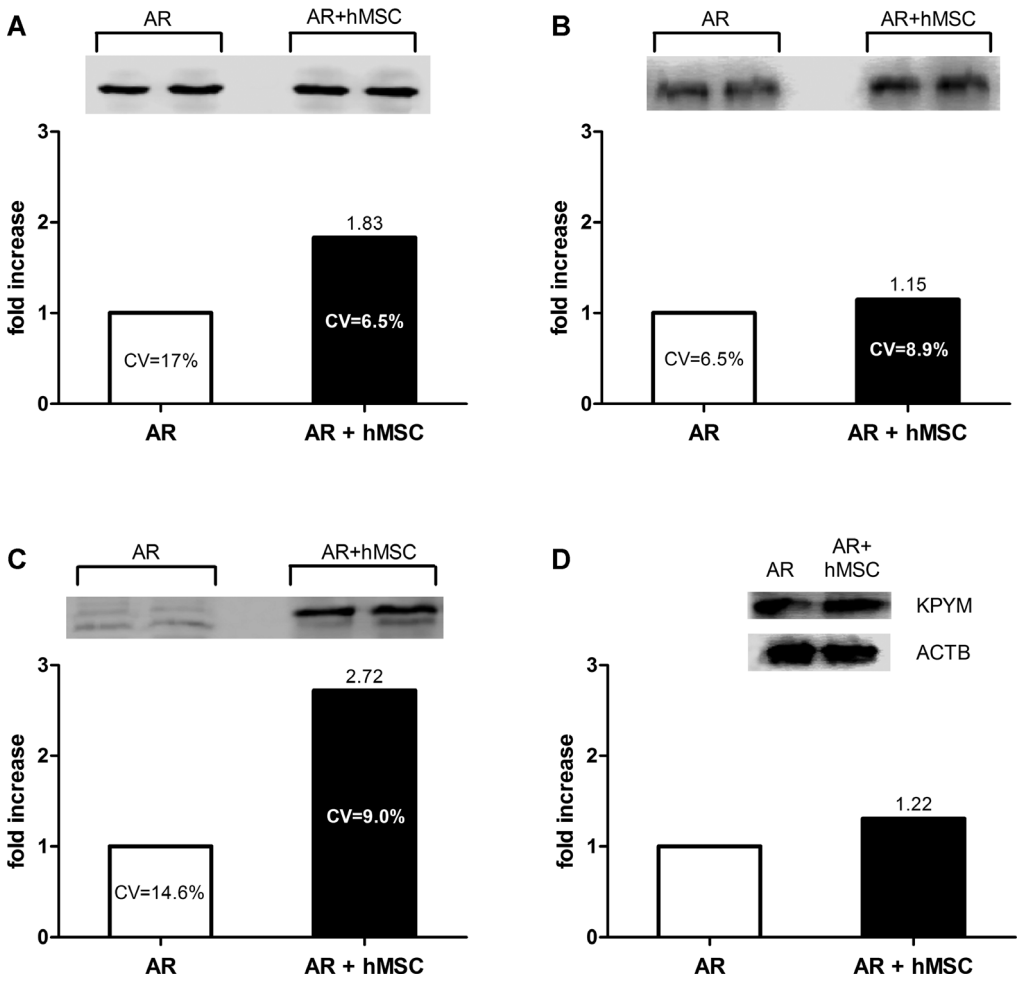


**Figure 6.** hMSC-induced increase of selected proteins, analyzed by Western blotting. Panels show representative immunostainings from the same gel and the fold increase of abundance in HK-2 exposed to hMSC, calculated from the different replicates, with the AR condition as reference. The conditions are indicated on the abscissae. (A) ATPB, FoF1-ATP synthase β subunit. (B) MDHM, malate dehydrogenase. (C) PRDX6, peroxiredoxin 6 isoform. (D) KPYM, pyruvate kinase. Immunoassays for ATPB, MDHM, and PRDX6 were carried out using three gels, each one containing lanes loaded with samples obtained in AR and AR + hMSC conditions. Different extract preparations were used for each gel. Absolute values of immunosignals in arbitrary units were used to calculate intraassay coefficients of variation (CV) among replicates, mean values being shown within the bars. (D) Single run of immunoanalysis for KPYM in which the AR and AR + hMSC conditions were assayed in the same gel. β-Actin was used in this case as a control for protein loading, using the sc-47778 antibody (1:1000 dilution, Santa Cruz Biotechnology, Santa Cruz, CA, USA). AR: HK-2 cells treated with antimycin A to block mitochondrial respiration and ATP synthesis followed by a 3-h recovery period; AR + hMSC: HK-2 cells treated with antimycin A, washed and cocultured with hMSC during the 3-h recovery period.

membrane potential. Thus, the following question emerged: do mesenchymal cells also upregulate enzymes involved in glycolysis and the Krebs cycle? The answer is yes. Some of the enzymes critical in energy metabolism are increased after exposure of renal cells to indirect contact with hMSC. Among these, the convergent upregulation of pyruvate kinase and L-lactate dehydrogenase at the end of the glycolytic pathway (Supporting Information Table S3), contributing to increased availability of pyruvate, seems to be strategically important from the perspective of cell survival when circulation and oxygenation recover after AKI. Moreover, extrapolating these findings to humans, the increased level of lactate dehydrogenase when $O_2$ is restored could help to clear the high plasma levels of L-lactate that frequently accompany AKI [55].

Another remarkable effect of hMSC detected through proteomic analysis is the increased expression of different proteins involved in cytoskeletal regulation and protein synthesis pathways in general (Fig. 2B and C). Organization of the actin cytoskeleton is essential for cell-to-cell and extracellular matrix adhesions and for preserving cell polarization, so it plays a central role in epithelial cell function. One consequence of ATP depletion is disruption of the actin cytoskeleton [37]; therefore it is reasonable to suppose that the protective

 

effect of hMSC interferes with cytoskeletal dynamics. The improvement of tubule architecture and functional parameters following stem cell administration has been demonstrated in an in vivo model of AKI [22], and our proteomic analysis indicates that this effect is mediated by the upregulation of actin-binding proteins, e.g. septin 7, filamin, profilin, and cofilin 1 and 2. Septin family proteins contribute to polarity and asymmetry in epithelial cells [56], which are crucial for normal vectorial transport of fluid through renal tubule cells. Filamin family proteins are important organizers of the cytoskeleton, and they contribute to membrane stabilization and act as signaling scaffolds and anchors for transmembrane proteins [57]. In addition to their role in the polymerization of actin monomers [58], profilin, and cofilin participate in energy homeostasis during ATP depletion [57, 59–61]. An additional role of cofilin is the chaperoning of actin to the nucleus, which can stimulate gene transcription [62], accelerating the cell cycle during recovery from AKI. This correlates closely with the upregulation of the 14–3–3 protein mentioned earlier (despite the problem of protein inference mentioned above regarding identification of isoforms), which has a clear role in maintaining the cell cycle (Supporting Information Fig. S5). Finally, the upregulation of several elongation and translation factors implicated in RNA expression and protein synthesis demonstrate that hMSC exposure leads to enhanced global protein synthesis, which is necessary to sustain their overall effects on cell growth, decreasing free radicals, and decelerating cell death.

The qRT-PCR data regarding key proteins linked to energy metabolism (Fig. 5A), cytoskeleton remodeling (Fig. 5B), and ROS handling (Fig. 5C) have an unexpected and apparently contradictory hallmark regarding the interaction of anoxic renal cells with hMSC during respiratory recovery. In most cases, the huge increase in mRNA after chemical anoxia emphasizes impaired translation, which seems to be released toward greater protein synthesis under the paracrine influence of hMSC during recovery. Uncontrolled accumulation of mRNA could—at least in part—be an effect of ATP depletion that leads to impaired translation, since ribosome biogenesis and translation are among the most energy-demanding processes in cells [63]. Indeed, it has already been demonstrated that global mRNA translation is intensely inhibited during hypoxia, but also that this inhibition is reversible [64, 65] and, most important, that the correlation between gene expression and protein expression is frequently poor [66, 67]. hMSC-induced abundance of proteins assayed by Western blotting does not quantitatively match the fold increase detected by MS. At first glance, this could be ascribed essentially to the different nature of the techniques. Although this is a limitation, the immunoassays support the view that—for the same proteins—proteomic data exhibit an opposite trend compared with qRT-PCR data, i.e. mRNA levels decrease (Fig. 5) as the abundance of protein rises (Fig. 6). Recovery of the intracellular ATP content (Fig. 4A) can be considered additional evidence that enzymes linked to energy metabolism are indeed more abundant in renal cells cocultured with hMSC. The discordance between protein abundance and mRNA levels, however, is far from being resolved and deserves further investigation.

It is noteworthy that the proteomic data were also validated by the functional data demonstrating decreased apoptosis, besides partial restoration of intracellular ATP content in HK-2 cells cocultured with hMSC. During the recovery period, soluble growth factors secreted by hMSC [9] as a result of a cross-talk with the injured renal cells [21] could interact with receptors on the HK-2 cell surface, triggering downstream signaling pathways that rapidly and ultimately switch on translation. The simultaneous restoration of ATP synthesis would provide the energy required for initiation, t-RNA/amino acid interaction, translation and termination of polypeptide chains [68]. It is also possible that simultaneous hMSC-induced upregulation of initiation and elongation factors in HK-2 cells (Supporting Information Table S3) synergizes with this stimulation of translation. Taken as a whole, these findings suggest that the effect of hMSC on renal cells is mediated mainly by the induction of protein translation—from the mRNA accumulated during anoxia—rather than transcription, a process made feasible by a parallel enhancement of ATP synthesis. This could explain the increased expression of the proteins we have investigated and the reduction of the corresponding mRNA in AR + hMSC cells.

The large-scale shotgun proteomic approach applied here provides a comprehensive view of events in injured renal cells during their interaction with hMSC, providing new insights into the molecular mechanisms involved. The possibility of quantitatively analyzing hundreds of proteins in a single experiment makes 2D-NanoUPLC tandem nanoESI-$MS^E$ a valuable tool for investigating complex phenomena such as–in this case–the mechanism of action of stem cells on renal cells. This contributes to a better understanding of the mechanisms of cell therapy in kidney diseases, which is vital for improving both efficacy and safety in clinical practice. Comprehension of the molecular mechanisms of the paracrine interactions between hMSC and injured targets in human tissues will improve safety and quality control of hMSC-based cell therapies. Currently, a growing number of clinical trials are being carried out in order to test the efficacy and safety of the infusion of hMSC to treat various clinical conditions (http://clinicaltrials.gov). MSC capacities to home to sites of injury and to secrete bioactive factors are considered some of the most important biological characteristics that enable them to exert therapeutic effects [69]. In this respect, the use of MSC conditioned medium instead of cell infusion is likely to recapitulate the regenerative effects, as previously demonstrated in kidney [47], liver [70], central nervous system [71], and heart [72]. These results certainly represent an opportunity to open a wide range of possibilities for clinical applications in more diseases, as recently emphasized [69]. Moreover, MSC from other sources such as umbilical cord or adipose tissue, which could deliver an ensemble of factors and extracellular vesicles differing in part from those secreted

by bone marrow-derived MSC, will shed additional light on the field of MSC-based cell therapies.

*We acknowledge the technical assistance of Glória Costa-Sarmento. This work was supported by grants from the Carlos Chagas Filho Research Foundation of the State of Rio de Janeiro (FAPERJ), the Brazilian National Research Council (CNPq), the Brazilian Federal Agency for Support and Evaluation of Graduate Education (CAPES), and the National Institutes of Science and Technology (INCT), Brazil.*

*The authors have declared no conflict of interest.*

## 5 References

[1] Portilla, D., Kaushal, G. P., Basnaldan, A. G., Shah, S. V., in: Runge, M. S., Patterson, C. (Eds.), *Principles of Molecular Medicine*, Humana Press, New Jersey 2006, pp. 643–649.

[2] Bonventre, J. V., Yang, L., Cellular pathophysiology of ischemic acute kidney injury. *J. Clin. Invest.* 2011, *121*, 4210–4221.

[3] Burt, R. K., Loh, Y., Pearce, W., Beohar, N. et al., Clinical applications of blood-derived and marrow-derived stem cells for nonmalignant diseases. *JAMA* 2008, *299*, 925–936.

[4] Tögel, F. E., Westenfelder, C., Kidney protection and regeneration following acute injury: progress through stem cell therapy. *Am. J. Kidney. Dis.* 2012, *60*, 1012–1022.

[5] Singer, N. G., Caplan, A. I., Mesenchymal stem cells: mechanisms of inflammation. *Annu. Rev. Pathol.* 2011, *6*, 457–478.

[6] Caplan, A. I., Why are MSCs therapeutic? New data: new insight. *J. Pathol.* 2009, *217*, 318–324.

[7] Rosenbaum, A. J., Grande, D. A., Dines, J. S., The use of mesenchymal stem cells in tissue engineering: a global assessment. *Organogenesis* 2008, *4*, 23–27.

[8] Costa, M. R., Verdoorn, K. S., Lindoso, R. S., Einicker-Lamas, M. et al., in: Goldenberg, R. C. S., Carvalho, A. C. C. (Eds.), *Resident Stem Cells and Regenerative Therapy*, Academic Press, Massachusetts 2012, pp. 1–31.

[9] Humphreys, B. D., Bonventre, J. V., Mesenchymal stem cells in acute kidney injury. *Annu. Rev. Med.* 2008, *59*, 311–325.

[10] Reis, L. A., Borges, F. T., Simoes, M. J., Borges, A. A. et al., Bone marrow-derived mesenchymal stem cells repaired but did not prevent gentamicin-induced acute kidney injury through paracrine effects in rats. *PLoS One* 2012, *7*, e44092.

[11] Tomasoni, S., Longaretti, L., Rota, C., Morigi, M. et al., Transfer of growth factor receptor mRNA via exosomes unravels the regenerative effect of mesenchymal stem cells. *Stem. Cells. Dev.* 2013, *22*, 772–780.

[12] Xinaris, C., Morigi, M., Benedetti, V., Imberti, B. et al., A novel strategy to enhance mesenchymal stem cell migration capacity and promote tissue repair in an injury specific fashion. *Cell. Transplant.* 2013, *22*, 423–436.

[13] Duffield, J. S., Park, K. M., Hsiao, L. L., Kelley, V. R. et al., Restoration of tubular epithelial cells during repair of the postischemic kidney occurs independently of bone marrow-derived stem cells. *J. Clin. Invest.* 2005, *115*, 1743–1755.

[14] Humphreys, B. D., Valerius, M. T., Kobayashi, A., Mugford, J. W. et al., Intrinsic epithelial cells repair the kidney after injury. *Cell. Stem. Cell.* 2008, *2*, 284–291.

[15] Tögel, F., Hu, Z., Weiss, K., Isaac, J. et al., Administered mesenchymal stem cells protect against ischemic acute renal failure through differentiation-independent mechanisms. *Am. J. Physiol. Renal. Physiol.* 2005, *289*, F31–42.

[16] Meirelles Lda, S., Fontes, A. M., Covas, D. T., Caplan, A. I., Mechanisms involved in the therapeutic properties of mesenchymal stem cells. *Cytokine. Growth. Factor. Rev.* 2009, *20*, 419–427.

[17] Du Rocher, B., Mencalha, A. L., Gomes, B. E., Abdelhay, E., Mesenchymal stromal cells impair the differentiation of CD14(++) CD16(–) CD64(+) classical monocytes into CD14(++) CD16(+) CD64(++) activate monocytes. *Cytotherapy* 2012, *14*, 12–25.

[18] Dagher, P. C., Modeling ischemia in vitro: selective depletion of adenine and guanine nucleotide pools. *Am. J. Physiol. Cell. Physiol.* 2000, *279*, C1270–C1277.

[19] Russ, A. L., Haberstroh, K. M., Rundell, A. E., Experimental strategies to improve in vitro models of renal ischemia. *Exp. Mol. Pathol.* 2007, *83*, 143–159.

[20] Kumar, S., Allen, D. A., Kieswich, J. E., Patel, N. S. et al., Dexamethasone ameliorates renal ischemia-reperfusion injury. *J. Am. Soc. Nephrol.* 2009, *20*, 2412–2425.

[21] Lindoso, R. S., Araujo, D. S., Adao-Novaes, J., Mariante, R. M. et al., Paracrine interaction between bone marrow-derived stem cells and renal epithelial cells. *Cell. Physiol. Biochem.* 2011, *28*, 267–278.

[22] Beiral, H. J., Rodrigues-Ferreira, C., Fernandes, A. M., Gonsalez, S. R. et al., The impact of stem cells on electron fluxes, proton translocation and ATP synthesis in kidney mitochondria after ischemia/reperfusion. *Cell. Transplant.* 2014, *23*, 207–220.

[23] Pizzatti, L., Panis, C., Lemos, G., Rocha, M. et al., Label-free MSE proteomic analysis of chronic myeloid leukemia bone marrow plasma: disclosing new insights from therapy resistance. *Proteomics.* 2012, *12*, 2618–2631.

[24] Mbeunkui, F., Goshe, M. B., Investigation of solubilization and digestion methods for microsomal membrane proteome analysis using data-independent LC-MSE. *Proteomics* 2011, *11*, 898–911.

[25] Panis, C., Pizzatti, L., Herrera, A. C., Cecchini, R., Abdelhay, E., Putative circulating markers of the early and advanced stages of breast cancer identified by high-resolution label-free proteomics. *Cancer Lett.* 2013, *330*, 57–66.

[26] Liu, H., Finch, J. W., Luongo, J. A., Li, G. Z., Gebler, J. C., Development of an online two-dimensional nanoscale liquid chromatography/mass spectrometry method for improved chromatographic performance and hydrophobic peptide recovery. *J. Chromatogr. A* 2006, *1135*, 43–51.

[27] Silva, J. C., Denny, R., Dorschel, C. A., Gorenstein, M. et al., Quantitative proteomic analysis by accurate mass retention time pairs. *Anal. Chem.* 2005, *77*, 2187–2200.

[28] Silva, J. C., Gorenstein, M. V., Li, G. Z., Vissers, J. P., Geromanos, S. J., Absolute quantification of proteins by LCMSE:

 

a virtue of parallel MS acquisition. *Mol. Cell. Proteomics* 2006, *5*, 144–156.

[29] Geromanos, S. J., Hughes, C., Golick, D., Ciavarini, S. et al., Simulating and validating proteomics data and search results. *Proteomics* 2011, *11*, 1189–1211.

[30] Li, G. Z., Vissers, J. P., Silva, J. C., Golick, D. et al., Database searching and accounting of multiplexed precursor and product ion spectra from the data independent analysis of simple and complex peptide mixtures. *Proteomics* 2009, *9*, 1696–1719.

[31] Spielmann, H., Jacob-Müller, U., Schulz, P., Simple assay of 0.1–1.0 pmol of ATP, ADP, and AMP in single somatic cells using purified luciferin luciferase. *Anal. Biochem.* 1981, *113*, 172–178.

[32] Lieberthal, W., Koh, J. S., Levine, J. S., Necrosis and apoptosis in acute renal failure. *Semin. Nephrol.* 1998, *18*, 505–518.

[33] Choudhary, C., Mann, M., Decoding signalling networks by mass spectrometry-based proteomics. *Nat. Rev. Mol. Cell. Biol.* 2010, *11*, 427–439.

[34] Cortezzi, S. S., Garcia, J. S., Ferreira, C. R., Braga, D. P. et al., Secretome of the preimplantation human embryo by bottom-up label-free proteomics. *Anal. Bioanal. Chem.* 2011, *401*, 1331–1339.

[35] Geromanos, S. J., Vissers, J. P., Silva, J. C., Dorschel, C. A. et al., The detection, correlation, and comparison of peptide precursor and product ions from data independent LC-MS with data dependant LC-MS/MS. *Proteomics* 2009, *9*, 1683–1695.

[36] Blackburn, K., Mbeunkui, F., Mitra, S. K., Mentzel, T., Goshe, M. B., Improving protein and proteome coverage through data-independent multiplexed data-independent multiplexed peptide fragmentation. *J. Proteome. Res.* 2010, *9*, 3621–3637.

[37] Sharfuddin, A. A., Molitoris, B. A., Pathophysiology of ischemic acute kidney injury. *Nat. Rev. Nephrol.* 2011, *7*, 189–200.

[38] Lau, R., Pratt, M. A., The opposing roles of cellular inhibitor of apoptosis proteins in cancer. *ISRN Oncol.* 2012, *2012*, 928120.

[39] Shi, Y., Mechanisms of caspase activation and inhibition during apoptosis. *Mol. Cell.* 2002, *9*, 459–470.

[40] Wang, C. Y., Mayo, M. W., Korneluk, R. G., Goeddel, D. V., Baldwin, A. S., Jr., NF-kappaB antiapoptosis: induction of TRAF1 and TRAF2 and c-IAP1 and c-IAP2 to suppress caspase-8 activation. *Science* 1998, *281*, 1680–1683.

[41] Nurmi, A., Lindsberg, P. J., Koistinaho, M., Zhang, W. et al., Nuclear factor-kappaB contributes to infarction after permanent focal ischemia. *Stroke* 2004, *35*, 987–991.

[42] Jin, J., Smith, F. D., Stark, C., Wells, C. D. et al., Proteomic, functional, and domain-based analysis of in vivo 14–3–3 binding proteins involved in cytoskeletal regulation and cellular organization. *Curr. Biol.* 2004, *14*, 1436–1450.

[43] Bustos, D. M., The role of protein disorder in the 14–3–3 interaction network. *Mol. Biosyst.* 2012, *8*, 178–184.

[44] van Hemert, M. J., Steensma, H. Y., van Heusden, G. P., 14–3–3 proteins: key regulators of cell division, signalling and apoptosis. *Bioessays* 2001, *23*, 936–946.

[45] Zha, J., Harada, H., Yang, E., Jockel, J., Korsmeyer, S. J., Serine phosphorylation of death agonist BAD in response to survival factor results in binding to 14–3–3 not BCL-X(L). *Cell* 1996, *87*, 619–628.

[46] Datta, S. R., Katsov, A., Hu, L., Petros, A. et al., 14–3–3 proteins and survival kinases cooperate to inactivate BAD by BH3 domain phosphorylation. *Mol. Cell* 2000, *6*, 41–51.

[47] Tögel, F., Weiss, K., Yang, Y., Hu, Z. et al., Vasculotropic, paracrine actions of infused mesenchymal stem cells are important to the recovery from acute kidney injury. *Am. J. Physiol. Renal. Physiol.* 2007, *292*, F1626–F1635.

[48] Thimmaiah, K. N., Easton, J. B., Houghton, P. J., Protection from rapamycin-induced apoptosis by insulin-like growth factor-I is partially dependent on protein kinase C signaling. *Cancer Res.* 2010, *70*, 2000–2009.

[49] Nath, K. A., Norby, S. M., Reactive oxygen species and acute renal failure. *Am. J. Med.* 2000, *109*, 665–678.

[50] Sengupta, R., Holmgren, A., Thioredoxin and thioredoxin reductase in relation to reversible S-nitrosylation. *Antioxid. Redox. Signal.* 2013, *18*, 259–269.

[51] Manevich, Y., Fisher, A. B., Peroxiredoxin 6, a 1-Cys peroxiredoxin, functions in antioxidant defense and lung phospholipid metabolism. *Free. Radic. Biol. Med.* 2005, *38*, 1422–1432.

[52] Szabo, C., Ischiropoulos, H., Radi, R., Peroxynitrite: biochemistry, pathophysiology and development of therapeutics. *Nat. Rev. Drug. Discov.* 2007, *6*, 662–680.

[53] Schwab, S. J., Klahr, S., Hammerman, M. R., Uptake of Pi in basolateral vesicles after release of unilateral ureteral obstruction. *Am. J. Physiol.* 1984, *247*, F543–547.

[54] Hinkle, P. C., P/O ratios of mitochondrial oxidative phosphorylation. *Biochim. Biophys. Acta.* 2005, *1706*, 1–11.

[55] Cerda, J., Tolwani, A. J., Warnock, D. G., Critical care nephrology: management of acid-base disorders with CRRT. *Kidney. Int.* 2012, *82*, 9–18.

[56] Bowen, J. R., Hwang, D., Bai, X., Roy, D., Spiliotis, E. T., Septin GTPases spatially guide microtubule organization and plus end dynamics in polarizing epithelia. *J. Cell. Biol.* 2011, *194*, 187–197.

[57] Feng, Y., Walsh, C. A., The many faces of filamin: a versatile molecular scaffold for cell motility and signalling. *Nat. Cell. Biol.* 2004, *6*, 1034–1038.

[58] Lee, S. H., Dominguez, R., Regulation of actin cytoskeleton dynamics in cells. *Mol. Cells.* 2010, *29*, 311–325.

[59] Atkinson, S. J., Hosford, M. A., Molitoris, B. A., Mechanism of actin polymerization in cellular ATP depletion. *J. Biol. Chem.* 2004, *279*, 5194–5199.

[60] Suurna, M. V., Ashworth, S. L., Hosford, M., Sandoval, R. M. et al., Cofilin mediates ATP depletion-induced endothelial cell actin alterations. *Am. J. Physiol. Renal. Physiol.* 2006, *290*, F1398–F1407.

[61] Bernstein, B. W., Bamburg, J. R., ADF/cofilin: a functional node in cell biology. *Trends Cell. Biol.* 2010, *20*, 187–195.

[62] Zheng, B., Han, M., Bernier, M., Wen, J. K., Nuclear actin and actin-binding proteins in the regulation of transcription and gene expression. *Febs. J.* 2009, *276*, 2669–2685.

 

[63] Proud, C. G., Signalling to translation: how signal transduction pathways control the protein synthetic machinery. *Biochem. J.* 2007, *403*, 217–234.

[64] Koumenis, C., Naczki, C., Koritzinsky, M., Rastani, S. et al., Regulation of protein synthesis by hypoxia via activation of the endoplasmic reticulum kinase PERK and phosphorylation of the translation initiation factor eIF2alpha. *Mol. Cell. Biol.* 2002, *22*, 7405–7416.

[65] Koritzinsky, M., Seigneuric, R., Magagnin, M. G., van den Beucken, T. et al., The hypoxic proteome is influenced by gene-specific changes in mRNA translation. *Radiother. Oncol.* 2005, *76*, 177–186.

[66] de Sousa Abreu, R., Penalva, L. O., Marcotte, E. M., Vogel, C., Global signatures of protein and mRNA expression levels. *Mol. Biosyst.* 2009, *5*, 1512–1526.

[67] Maier, T., Güell, M., Serrano, L., Correlation of mRNA and protein in complex biological samples. *FEBS. Lett.* 2009, *583*, 3966–3973.

[68] Marshall, R. A., Aitken, C. E., Dorywalska, M., Puglisi, J. D., Translation at the single-molecule level. *Annu. Rev. Biochem.* 2008, *77*, 177–203.

[69] Wang, S., Qu, X., Zhao, R. C., Clinical applications of mesenchymal stem cells. *J. Hematol. Oncol.* 2012, *5*, 19.

[70] van Poll, D., Parekkadan, B., Cho, C. H., Berthiaume, F. et al., Mesenchymal stem cell-derived molecules directly modulate hepatocellular death and regeneration in vitro and in vivo. *Hepatology* 2008, *47*, 1634–1643.

[71] Cantinieaux, D., Quertainmont, R., Blacher, S., Rossi, L., Conditioned medium from bone marrow-derived mesenchymal stem cells improves recovery after spinal cord injury in rats: an original strategy to avoid cell transplantation. *PLOS One* 2013, *8*, e69515.

[72] Timmers, L., Lim, S. K., Hoefer, I. E., Arslan, F. et al., Human mesenchymal stem cell-conditioned medium improves cardiac function following myocardial infarction. *Stem. Cell Res.* 2011, *6*, 206–214.

 